Asian Journal of Chemical and Pharmaceutical Research
CODEN (USA):AJCPHP | ISSN: 2347-8322 |Publisher: Pharma Research Library
Home Page: https://pharmaresearchlibrary.org/journals/index.php/ajcpr
DOI: https://doi.org/10.30904/j.ajcpr.2025.4770
A. J. Chem. Pharm, Res., 2025, 13(1): 24-32

Design, Synthesis, Characterization, and Analysis of Antimicrobial Property of Novel Benzophenone Fused Azetidinone Derivatives through *In-Silico* Approach

M Murali Naik*[1], Ghantasala Nirupama[2], P. Akhila Swathanthra[3], Anke Rajasekhar Babu[1], V Ramanjineyulu[1]

[1]Department of Chemical Engineering, JNTUACEA, JNTUA, Anantapuramu, Andhra Pradesh, India
[2]Department of Civil Engineering, JNTUACEA, JNTUA, Anantapuramu, Andhra Pradesh, India
[3]Department of Chemical Engineering, SVUCE, SVU, Tirupati, Andhra Pradesh, India

A B S T R A C T

A sequence of novel 2-(4-benzoyl-2-methyl-phenoxy)-N-(3-chloro-2-oxo-4-phenyl-azetidin-1-yl)-acetamide analogues 9(a–n) were synthesized through a multistep process. The newly developed compounds were thoroughly characterized, and their antimicrobial activities were evaluated using disc diffusion and broth dilution methods. Additionally, all compounds in the series (9a–n) were tested against various bacterial and fungal strains, with Ketoconazole, Chloramphenicol, and Amoxicillin serving as reference drugs. Among them, compounds 9a, 9e, and 9g exhibited significant inhibition against the tested strains. Furthermore, molecular docking studies were conducted on the most potent compounds to analyze their three-dimensional geometric interactions with target proteins.

Keywords: 2-Azetidinone, benzophenone, antimicrobial, insilico, molecular docking simulations.

A R T I C L E I N F O

***Corresponding Author**
M Murali Naik
Department of Chemical Engineering,
JNTUACEA, JNTUA,
Anantapuramu, Andhra Pradesh, India.
E-mail: muralinaik117@gmail.com

Article History:
Received : 10 Oct 2024
Revised : 30 Oct 2024
Accepted : 12 Dec 2024
Published : 09 Jan 2025

Citation: *M Murali Naik, et al. Design, Design, Synthesis, Characterization, and Analysis of Antimicrobial Property of Novel Benzophenone Fused Azetidinone Derivatives through In-Silico Approach. A. J. Chem. Pharm, Res., 2025, 13(1): 24-32.*

C o n t e n t s

1. Introduction

For several years, the rise of microorganisms resistant to nearly all classes of antimicrobial agents have become a significant public health concern. The discovery and design of new antimicrobial drugs have been a primary focus for researchers in the pursuit of more effective treatments. In recent decades, the issue of multidrug-resistant microorganisms has reached alarming levels worldwide. The World Health Organization (WHO) has identified antimicrobial resistance (AMR) as one of the top ten global public health threats. In the United States alone, over 2.8 million antibiotic-resistant infections occur annually, leading to more than 35,000 deaths. Additionally, in 2017, approximately 223,900 individuals required hospitalization due to Clostridioides difficile, with at least 12,800 fatalities reported [1-4]. Resistance to multiple antimicrobial agents, including β-lactam antibiotics, macrolides, quinolones, and vancomycin, has been documented. Moreover, numerous clinical reports highlight the increasing prevalence of methicillin-resistant Staphylococcus aureus (MRSA), drug-resistant Streptococcus pneumoniae, carbapenem-resistant Enterobacteriaceae (CRE), erythromycin-resistant group A Streptococcus, and clindamycin-resistant group B

Streptococcus, all of which contribute to severe infections, particularly in developed countries [5,6]. In addition to bacterial resistance, systemic fungal infections have become a growing concern. The first orally active antifungal agent, ketoconazole, proved effective against a wide range of systemic and superficial fungal infections. Since then, several azole antifungal agents, such as itraconazole, fluconazole, voriconazole, and ravuconazole, as well as the glucan synthesis inhibitor caspofungin, have been introduced into clinical practice.

Antibiotics have played a crucial role in combating bacterial infections and improving public health. However, their effectiveness is diminishing due to increasing bacterial resistance and associated toxicity concerns [7,8]. The rise of drug-resistant infections presents a significant challenge to the medical community, necessitating the search for novel antimicrobial agents with reduced resistance.

2-Azetidinone, a four-membered heterocyclic amide commonly known as β-lactam, is widely recognized for its structural presence in broad-spectrum β-lactam antibiotics, including penicillins, cephalosporins, carbapenems, and monobactams. These compounds have been extensively utilized as chemotherapeutic agents for bacterial and microbial infections. Beyond their biological properties, β-lactams also serve as crucial synthetic intermediates in organic synthesis, such as in the semi-synthesis of Taxol. Similarly, benzophenone analogues have demonstrated significant potential as anticancer, anti-inflammatory, and antimicrobial agents [9-12].

In view of these factors, we designed and synthesized hybrid molecules combining benzophenone with an azetidinone moiety. The antimicrobial and antifungal activities of these newly developed compounds were further analyzed through in silico docking simulations [15,16]. The targets for antimicrobial docking studies were selected based on literature highlighting β-lactams as potent inhibitors of transpeptidases, a crucial enzyme class in bacterial cell wall synthesis. Likewise, antifungal targets were chosen based on evidence that azetidinones effectively inhibit CYP51 and other P450 enzymes in fungi. The inhibition of these enzymes disrupts fungal membrane integrity by accumulating methylated sterol precursors of ergosterol, similar to the action of ketoconazole, which was used as a reference drug in invitro studies [17-20].

2. Methodology

All solvents and reagents were procured from Sigma Aldrich Chemicals Pvt. Ltd., India. Melting points were measured using an electrically heated VMP-III melting point apparatus. FT-IR spectra were recorded on an FT-IR Jasco 4100 infrared spectrophotometer using KBr discs and Nujol. The ^{1}H NMR spectra were obtained on a Bruker DRX 400 spectrometer at 400 MHz, with TMS as the internal standard. Mass spectra were recorded using an LC-MS (API-4000) mass spectrometer. Additionally, elemental analysis of the compounds was conducted using a Perkin Elmer 2400 elemental analyzer.

General Procedure for the Synthesis of Phenyl Benzoates 3(a–b): Substituted benzoates 3(a–b) were prepared by benzoylating o-cresol (1, 0.001mol) with the respective benzoyl chlorides 2(a–b) (0.001mol) in the presence of a 10% sodium hydroxide solution. The reaction mixture was stirred at 0°C for 2–3 hours and monitored using thin-layer chromatography (TLC) with an n-hexane: ethyl acetate (4:1) solvent system [21,22]. Upon completion, the organic layer was extracted with ether (3 × 15 mL), washed with 10% sodium hydroxide solution (3 × 30 mL) and water (3 × 25 mL), then dried over anhydrous sodium sulfate. The solvent was evaporated, and the resulting solid was recrystallized from ethanol to obtain pure compounds 3(a–b). Characterization data are provided in the Supplementary File [23,24].

General Procedure for the Synthesis of Substituted 4-Hydroxy Benzophenones 4(a–b)

Substituted 4-hydroxy benzophenones 4(a–b) were synthesized via the Fries rearrangement. Compounds 3(a–b) (0.001 mol) were treated with anhydrous aluminum chloride (0.002 mol) as a catalyst and heated at 150–170°C under neat conditions for 2–3 hours. After cooling to room temperature, the reaction mixture was quenched with 6N HCl in the presence of ice-cold water and stirred for 2–3 hours. The resulting solid was filtered and recrystallized from ethanol to obtain pure compounds 4(a–b) [25-27].

General Procedure for the Synthesis of Ethyl 2-(4-Benzoyl-2-Methylphenoxy) Acetates 5(a–b)

Compounds 5(a–b) were synthesized by refluxing a mixture of compounds 4(a–b) (0.013 mol) and ethyl chloroacetate (0.026 mol) in dry acetone (35 mL) with anhydrous potassium carbonate (0.019 mol) as a weak base for 8–9 hours. After cooling, the solvent was removed by distillation, and the residue was triturated with cold water to eliminate potassium carbonate. The mixture was extracted with ether (3 × 50 mL), and the ether layer was washed with 10% sodium hydroxide solution (3 × 50 mL) and water (3 × 30 mL), then dried over anhydrous sodium sulfate. Evaporation of the solvent yielded a crude solid, which was recrystallized from ethanol to obtain pure compounds 5(a–b) [28,29].

General Procedure for the Synthesis of Substituted 2-(4-Benzoyl-2-Methylphenoxy) Acetohydrazides 6(a–b)

To a solution of compounds 5(a–b) (0.01 mol) in ethanol (10 mL), 99% hydrazine hydrate (0.01 mol) was added dropwise while stirring continuously at room temperature for 2 hours. The resulting white solid was filtered and recrystallized from methanol to obtain pure compounds 6(a–b) [30,31].

General Procedure for the Synthesis of Substituted 2-(4-Benzoyl-2-Methylphenoxy)-N Benzylideneacetohydrazides 8(a–n)

A solution of compounds 6(a–b) (0.01 mol) in absolute ethanol (50 mL) was combined with a catalytic amount of acetic acid and an equimolar quantity of the corresponding aldehydes 7(a–g). The reaction mixture was refluxed for 8–10 hours, then cooled to room temperature, poured onto crushed ice, filtered, washed, dried, and recrystallized from acetonitrile to obtain compounds 8(a–n) in good yield [32-34].

General Procedure for the Synthesis of 2-(4-Benzoyl-2-Methylphenoxy)-N-(3-Chloro-2-Oxo-4-Phenylazetidin-1-yl)-Acetamides 9(a–n): A solution of compounds 8(a–n) (0.01mol) and triethylamine (0.01mol) in dioxane (50 mL) was cooled and stirred. To this well-stirred, chilled solution, chloroacetyl chloride (0.01mmol) was added drop wise over 20 minutes. The reaction mixture was then stirred for an additional 3 hours and allowed to stand at room temperature for 48hr. After completion, the mixture was concentrated, cooled, and poured into ice-cold water. The resulting solid was filtered, dried, and purified by column chromatography over silica gel using a 30% ethyl acetate: 70% benzene solvent system. Recrystallization from a suitable solvent yielded pure 2-azetidinone derivatives 9(a–n) [35-40].

Pharmacology

Docking Simulation (Methodology)

Molecular docking simulations were performed using AutoDock Tools version 4 (ADT4) [41]. The structural data for the target proteins—5E1G for antibacterial studies and 3LD6 for antifungal studies—were obtained from the RCSB PDB database (http://www.rcsb.org/pdb/, accessed on 5 February 2025). These proteins were selected based on literature reports indicating that β-lactam and azetidinone derivatives are potent inhibitors of microbial and fungal targets, making them promising candidates for antimicrobial and antifungal therapy [42-45]. Additionally, the synthesized compounds shared key substructural features with the co-crystal ligand of the target proteins, further justifying their selection for docking studies. Before performing the docking simulations, all co-crystal ligands, ions, and water molecules were removed from the protein structures. The proteins were then prepared by neutralizing charges, adding polar hydrogens, and defining rotatable bonds using ADT4 [46-49].

The ligand structures were generated using ChemDraw Ultra 12.0, energy-minimized with the MM2 force field, and saved in PDB format. Docking simulations for all ligands against the selected protein targets were conducted using the Lamarckian Genetic Algorithm (LGA) model [50], a widely employed method for predicting binding modes and conformations [51-53]. The grid was centered at the active site pocket of each protein with a grid box size of 120 × 120 × 120 Å³ and a grid-point spacing of 0.425 Å. Among all ligand-receptor interactions, compounds 9a, 9e, and 9g exhibited the highest binding affinity, forming significant hydrogen bonds. Table 1 presents the docking results for compounds 9a, 9e and 9g including key parameters such as binding energy, hydrogen bond interactions and ligand efficiency (LE) [47]. The ligand efficiency was calculated as the ratio of Gibbs free energy of binding (G) to the number of non-hydrogen atoms in the compound, mathematically expressed as:

$$LE = (G) / N$$

Where G represents the Gibbs free energy of binding and N denotes the number of heavy atoms in the compound. Using the thermodynamic equation for Gibbs free energy, $\Delta G = -RT \ln Ki$, and approximating Ki with IC50 (a less rigorous estimation), ligand efficiency (LE) can be determined using the following formula:

$$LE = 1.4 (pIC50) / N$$

In addition to ADT4, BIOVIA and PyMOL were also employed for visualizing and presenting the ligand-protein conformations [54,55].

3. Results and Discussion

Structure-Based Design:

A comprehensive literature review was conducted to highlight the significance of four-membered nitrogen-containing heterocyclic compounds, particularly azetidinones, as well as benzophenone analogues. The study revealed that researchers have reported outstanding antimicrobial activity in azetidinone derivatives. Additionally, several benzophenone analogues previously reported by our group have shown promising antimicrobial properties. Moreover, widely recognized antimicrobial drugs such as penicillins, cephalosporins, carbapenems, and monobactams contain a β-lactam ring (Figure 1). β-Lactam antibiotics currently represent the most extensively used class of antibacterial agents in the treatment of infectious diseases, accounting for 65% of all injectable antibiotic prescriptions in the United States (Figure 2).

Notably, the target compounds incorporate key pharmacophoric elements essential for antimicrobial activity, including a β-lactam ring, a distal benzoyl group, a lipophilic aryl group, and the donor nitrogen atom of the acetamide bridge. Additionally, the carbonyl oxygen of the lactam ring forms hydrogen bonding interactions with Arg144 and Tyr75, while the amide oxygen also interacts with Arg144. The substituted phenyl ring exhibits pi-cation interactions with Pro87, Asn89, Glu240, and Arg84 residues. Based on these insights, we designed new analogues incorporating N-CO and other pharmacophores crucial for antimicrobial activity (Figure 3).

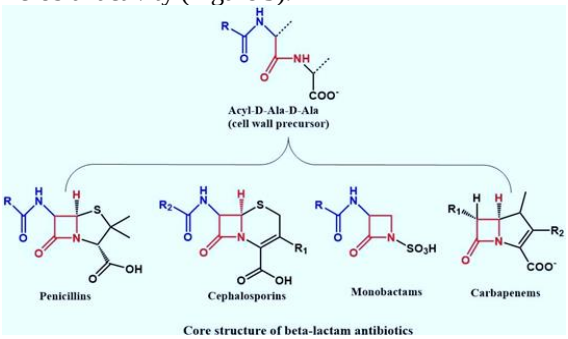

Figure 1. β-Lactam antibiotics

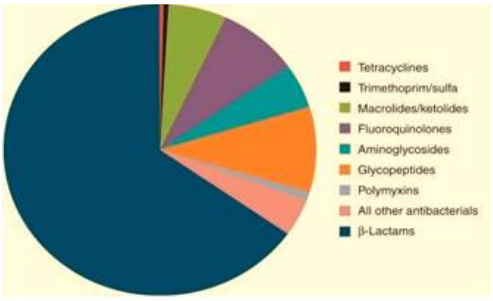

Figure 2. Proportion of prescriptions in the United States for injectable antibiotics by class for years 2004–2014.

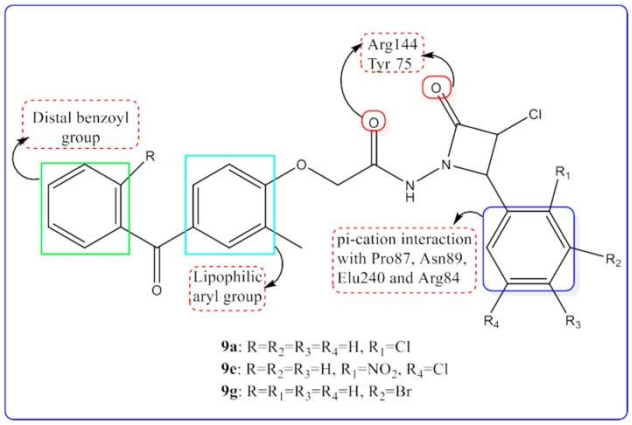

Figure 3. Design strategy

The synthesis of the title compounds 9(a–n) was carried out following the reaction sequence outlined in Scheme 1. All synthesized compounds were characterized using IR, NMR, and mass spectrometry. The starting materials, substituted phenyl benzoate analogues (3a–b), were prepared by the benzoylation of o-cresol (1) with the corresponding benzoyl chlorides 2(a–b) in the presence of 10% sodium hydroxide solution. These intermediates underwent Fries rearrangement under neat conditions using anhydrous aluminum chloride as a catalyst, yielding hydroxy benzophenones 4(a–b).

Etherification of compounds 4(a–b) with ethyl chloroacetate in dry acetone resulted in substituted ethyl 2-(4-benzoylphenoxy) acetates 5(a–b). These were then treated with hydrazine hydrate in ethanol under continuous stirring to obtain substituted 4-benzoyl-phenoxy aceto hydrazides 6(a–b). Subsequent treatment of compounds 6(a–b) with substituted aldehydes 7(a–g) in absolute ethanol, along with a catalytic amount of acetic acid, and refluxing for 8–10 hours, led to the formation of substituted 2-(4-benzoyl-2-methylphenoxy)-N-(2-benzylidene) acetohydrazides 8(a–n).

Finally, the compounds 8(a–n) were reacted with chloroacetyl chloride in dioxane using triethylamine as a catalyst. The reaction mixture was cooled and stirred, and chloroacetyl chloride was added dropwise over 20 minutes, followed by continued stirring for three hours, leading to the formation of the title compounds, substituted 2-(4-benzoyl-2-methyl-phenoxy)-N-(3-chloro-2-oxo-4-phenyl-azetidin-1-yl)-acetamides 9(a–n). To confirm the structure of the synthesized compounds, representative examples from each series were analyzed. Compound (3a) was characterized by the presence of a carbonyl stretching band for the ester group at 1715 cm^{-1} in the IR spectrum, nine aromatic protons between 7.0 and 7.8 ppm in the proton NMR spectrum, and a stable (M + 1) peak at m/z 213 in the mass spectrum.

Similarly, compound (4a) was confirmed by the disappearance of the ester carbonyl stretching band of compound (3a) in the IR spectrum, the presence of an OH stretching band at 3510–3600 cm^{-1}, a broad singlet for the OH proton at δ 12.0 ppm in the NMR spectrum, and a stable (M + 1) peak at m/z 213 in the mass spectrum.
Compound (5a) was identified by the appearance of the ester carbonyl stretching band at 1760 cm^{-1} in the IR spectrum, the disappearance of the OH proton singlet of compound (4a), and the presence of triplet and quartet peaks for CH_3 and CH_2 protons at δ 2.31 and 4.15 ppm, respectively, in the NMR spectrum. The mass spectrum showed a stable (M + 1) peak at m/z 299.

The formation of compound (6a) was confirmed by the presence of NH and NH_2 stretching bands at 3120–3220 cm^{-1} and an amide carbonyl stretching band at 1670 cm^{-1} in the IR spectrum. The proton NMR spectrum displayed a singlet peak for the amide −NH at δ 9.55 ppm and a singlet for NH_2, while the disappearance of triplet and quartet peaks for CH_3 and CH_2 from compound (5a) further confirmed the transformation. The mass spectrum exhibited a stable (M + 1) peak at m/z 286.

For compound (8a), the disappearance of the NH_2 band of compound (6a) and the appearance of a C=N stretching band at 1630 cm^{-1} in the IR spectrum, along with a singlet peak for the HC=N proton at δ 8.45 ppm and an increase in aromatic protons in the NMR spectrum, confirmed its formation. The mass spectrum revealed significant (M^+) and (M + 2) peaks at m/z 407 and 409, respectively.

Finally, compound (9a) was verified by the disappearance of the C=N stretching band from compound (8a) and the appearance of a carbonyl stretching band of the azetidinone ring at 1655 cm^{-1} in the IR spectrum. The proton NMR spectrum confirmed this with the disappearance of the HC=N singlet and the appearance of an N-CH singlet at δ 5.45 ppm and a Cl-CH singlet at δ 5.6 ppm. The mass spectrum exhibited significant peaks at m/z 483 (M^+) and 485 (M + 2), confirming the successful synthesis of compound (9a).

Molecular Docking Study

The antibacterial and antifungal activities of the synthesized compounds were predicted through in silico molecular docking studies using protein targets (PDB ID: 5E1G) for antibacterial and (PDB ID: 3LD6) for antifungal activity. Among all tested compounds, the docking results highlighted 9a, 9e, and 9g as the most promising candidates, exhibiting strong binding affinities and well-defined hydrogen bonding interactions with key amino acids within the active site pockets of the target proteins. Compound 9a displayed the best binding energy of −8.99 kcal/mol against the 5E1G protein, forming three hydrogen bonds with ligand efficiency and inhibition constant values of −0.27 and 2.14 μM, respectively (Table 4). In this binding conformation, the THR320 residue formed a hydrogen bond with the oxygen atom of the carbonyl group connecting the phenyl and phenoxy rings at a distance of 1.84 Å. Additionally, CYS354 and HIS336 established two hydrogen bonds with the oxygen atoms (=O and –O–) in the acetamide bridge at distances of 1.95 Å and 2.42 Å, respectively. Furthermore, the HIS352 residue exhibited

two pi-cation and pi-pi stacking interactions with the phenoxy ring, along with another pi-cation interaction with the chlorophenyl ring (Figure 5). Other docking conformations of 9a with the 5E1G protein also demonstrated favorable results (Table 4).

Compound 9e exhibited remarkable binding interactions with both protein targets, achieving a strong binding energy of −11.57 kcal/mol with the 3LD6 protein. This interaction involved the formation of four hydrogen bonds, with ligand efficiency and inhibition constant values of −0.32 and 3.31 μM, respectively (Table 4). The shortest hydrogen bond in this complex was formed between the LYS156N residue and an oxygen atom of the nitro group at a distance of 1.67 Å. Another oxygen atom of the nitro group formed a hydrogen bond with TYR145 at a distance of 1.98 Å. Additionally, TYR131 and ARG382 residues contributed two hydrogen bonds with the oxygen atom attached to the azetidine moiety at distances of 1.80 Å and 2.47 Å, respectively. The phenyl ring also participated in two pi-pi stacking interactions with TRP239 and a pi-cation interaction with HIS236 (Figure 5). Further details of compound 9e's docking conformations with the 3LD6 protein are summarized in Table 4.

Additionally, compound 9e displayed significant binding affinity towards the 5E1G protein, with a best binding energy of −9.86 kcal/mol, forming five hydrogen bonds. The ligand efficiency and inhibition constant were recorded as −0.27 and 59.52 μM, respectively (Table 4). In this binding conformation, one of the oxygen atoms of the nitro group formed two hydrogen bonds with HIS352 at distances of 1.80 Å and 2.60 Å. Another oxygen atom from the nitro group established two hydrogen bonds with HIS336 and ASN356 residues at distances of 2.14 Å and 2.30 Å, respectively. Furthermore, the oxygen atom of the azetidine moiety formed the shortest hydrogen bond with THR320 at a distance of 1.69 Å. This conformation was further stabilized by a pi-pi stacking interaction between the centroid of the chlorophenyl ring and TRP340 (Figure 5). Other docking conformations of compound 9e with the 5E1G protein are listed in Table 4.

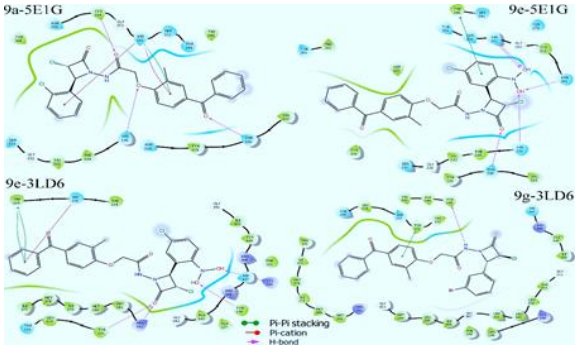

Figure 4. 2D interaction plots of the ligands at the active site of the proteins showing pi- cation and hydrogen bond interactions.

For the docking results of compound 9g with the 3LD6 protein, the best conformation exhibited a ligand efficiency of −0.31 and an inhibition constant of 27.82 μM, with a binding energy of −10.31 kcal/mol. This conformation featured a single hydrogen bond between the TYR145 residue and the nitrogen atom in the acetamide group at a distance of 2.04 Å. Additionally, a pi-pi stacking interaction was observed between the TYR131 residue and the centroid of the phenoxy ring (Figure 4). The parameters for all other docking conformations of compound 9g with the 3LD6 protein are summarized in Table 1.

Thus, compounds 9a and 9e fit well into the binding pocket of the 5E1G protein, interacting with several hydrophobic residues, hydrogen bonds, and pi contacts involving key amino acids such as TYR308, TYR318, THR320, GLY332, VAL333, PHE334, HIS336, TRP340, SER351, HIS352, GLY353, CYS354, and ASN356. These interactions closely resemble those observed in the cocrystallized ligand and other known 5E1G inhibitors.

Similarly, compounds 9e and 9g were well accommodated within the active site of the 3LD6 protein, forming multiple hydrogen bonds, hydrophobic interactions, and pi contacts with key residues including TYR131, LEU134, TYR145, THR135, PHE152, LYS156, HIS236, TRP239, ILE377, MET380, MET381, ARG382, HIS447, CYS449, and MET487. These interactions are analogous to those observed with the original 3LD6 protein inhibitor.

Figure 6 provides three-dimensional representations of the ligand-protein complexes, offering a detailed view of how the ligands are positioned within the active site groove of the proteins. Additionally, Figure 7 illustrates the ribbon model of the protein targets with the ligands depicted in a ball-and-stick representation for the most stable conformations.

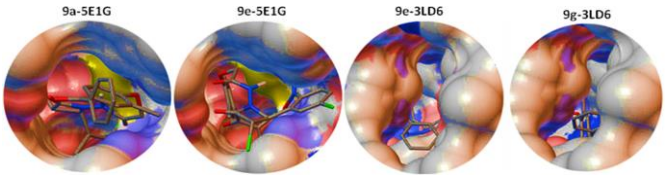

Figure 5. 3-D close view visualization of the ligand-protein complexes showing the enfolding f the ligands in the active site groove of the proteins.

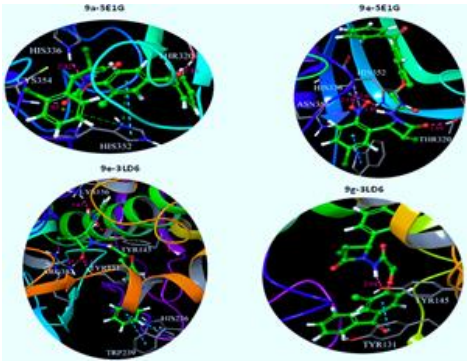

Figure 6. Ball and stick representation of the ligands with ribbon model of the protein targets showing hydrogen bond as dashed lines.

The docking simulations were validated by redocking the original inhibitors and co-crystal ligands with the same proteins, showing strong overlap with our ligands. The RMSD values for 9a and 9e docked with 5E1G were 0.172 and 0.201, respectively (Figure 8a), while 9e and 9g docked with 3LD6 had RMSD values of 0.182 and 0.216, respectively (Figure 8b). The in silico docking results aligned with experimental findings, highlighting the significance of the acetamide group, azetidinone, and phenyl ring in the biological activity of these compounds as potential antibacterial and antifungal agents.

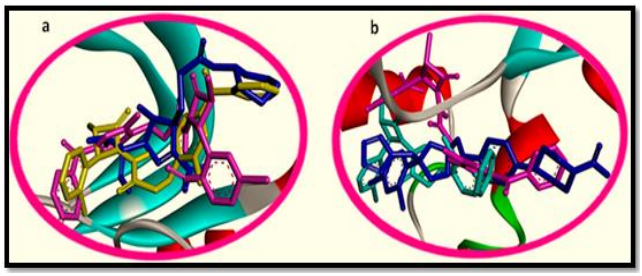

Figure 7. Overlapping of cocrystal ligands (blue color) with our synthesized compounds, 9a (yellow color), 9e (purple color) and 9g (cyan color) docked with; (a) 5E1G and (b) 3LD6 proteins.

Table 1. Results of in silico docking studies for 9a, 9e and 9g ligands with 3U2K, antibacterial, and 1JIP, antifungal, targets

Conf No.	Ligand	Protein	B.E (kcal/mol)	L.E	IC_{50} (µM)	vdW-HB-Des-Energy (kcal/mol)	HB of Residues and Ligands with Bond Length (Å)	Pi Interactions (Å)	RMSD
1	9a	SEIG	-9.99	-0.27	2.14	-10.99	THR320:N-HO (1.85), CYS385:N-HO (1.95)	HIS352-Cg2 (3.92)	0.172
1	9e	3LD6	-9.86	-0.27	59.52	-11.98	THR320:OH-O (2.00), HIS323:N-HO (1.91)	TRP540-Cg1 (3.59)	0.201
2	9a	SEIG	-11.57	-0.32	3.31	-12.07	LYS156:N-HO (1.8), TYR318:N-HO (1.9)	HIS326-Cg3 (3.96)	0.218
2	9g	3LD6	-10.31	-0.31	27.22	-12.42	TYR313:N-HO (2.3), ARG438:N-HO (2.4)	TRP329-Cg3 (3.32)	0.214
3	9a	SEIG	-8.67	-0.26	644.19	-11.08	THR320:OH-O (2.0), HIS323:N-HO (1.9)	TYR318-Cg2 (2.25)	1.311
3	9e	3LD6	-9.81	-0.26	42.7	-12.06	HIS323:N-HO (2.0), THR320:OH-O (2.1)	TRP540-Cg1 (3.59)	0.865
4	9a	SEIG	-8.52	-0.26	566.15	-11.08	THR320:OH-O (2.0), TYR318:N-HO (2.0)	TYR318-Cg2 (3.8)	10.361
4	9g	3LD6	-9.57	-0.27	126.48	-12.04	LYS156:N-HO (2.0), HIS323:N-HO (2.1)	THR320-Cg2 (2.8)	3.352
5	9a	SEIG	-8.07	-0.22	1.21	-10.99	ASN386:N-HO (1.78)	THR320-Cg2 (2.77)	0.951
5	9g	3LD6	-9.38	-0.30	62.5	-11.89	PHE234-Cg3 (4.0)	LYS156-Cg2 (2.85)	1.392
6	9a	SEIG	-7.99	-0.29	5.39	-12.08	LYS156:N-HO (2.5)	TRP540-Cg1 (3.92)	3.334
6	9g	3LD6	-9.10	-0.28	13.85	-11.32	ILE399:N-HO (2.11)	TRP329-Cg3 (3.92)	3.319
7	9a	SEIG	-7.74	-0.26	256.46	-8.90	TYR313:N-HO (3.0)	TRP540-Cg1 (2.92)	8.952
7	9g	3LD6	-9.00	-0.25	39.54	-11.06	ILE305:N-HO (2.01)	TRP540-Cg1 (3.92)	9.612
8	9a	SEIG	-8.07	-0.27	316.41	-11.06	THR320:OH-O (2.17)	TYR318-Cg2 (2.8)	9.234
8	9g	3LD6	-9.10	-0.18	397.02	-10.26	LYS156:N-HO (2.16)	LEU316-Cg2 (2.5)	12.234
9	9a	SEIG	-7.15	-	1.64	-7.97	HIS352:N-HO	TRP540-Cg2	11.381

				0.18			(1.67), ASN386:N-HO (1.67)	(4.00)	
9	9e	3LD6	-5.15	-0.15	16.1	-7.18	TRP319:N-HO (1.43)	HIS352-Cg2 (2.91)	14.918
10	9a	SEIG	-6.05	-0.18	50.95	-10.31	HIS352:N-HO (1.19), ASN386:N-HO (1.66)	TRP540-Cg1 (3.92)	4.035
10	9g	3LD6	-7.66	-0.23	2.43	-9.78	GLY446:N-HO (2.91)	ILE430-Cg2 (2.92)	0.744

4. Conclusion

In conclusion, a series of benzophenone-fused azetidinone derivatives were successfully synthesized through a multi-step process. The structural confirmation of all synthesized compounds was carried out. Additionally, these newly developed derivatives were evaluated for their antibacterial and antifungal activities. *Insilico* docking results aligned with the experimental findings, emphasizing the crucial role of the acetamide group, azetidinone, and phenyl ring in the biological activity of these compounds as potential antibacterial and antifungal agents.

5. References

[1] Khanum, S.A.; Shashikanth, S.; Sudha, B.S. A Facile Synthesis and Antimicrobial Activity of 3-(2-Aroylaryloxy) methyl-5- Mercapto-4-Phenyl-4H-1,2,4-Triazole and 2-(2-Aroylaryloxy) methyl-5-N-Phenylamino-1,3,4-Thiadiazole Analogues. *Sci. Asia* **2003**, *34*, 383–392.

[2] CDC. *Antibiotic Resistance Threats in the United States, 2019*; U.S. Department of Health and Human Services, CDC: Atlanta, GA, USA, 2019.

[3] Francis, J.S.; Doherty, M.C.; Lopatin, U.; Johnston, C.P.; Sinha, G.; Ross, T.; Cai, M.; Hanse, N.N.; Per, T.; Ticehurst, J.R.; et al. Severe community-onset pneumonia in healthy adults caused by methicillin-resistant Staphylococcus aureus carrying the Panton-Valentine leukocidin genes. *Clin. Infect. Dis.* **2005**, *40*, 100–107.

[4] Kruszewska, D.; Sahl, H.G.; Bierbaum, G.; Pag, U.; Hynes, S.O.; Ljungh, A. Mersacidin eradicates methicillin-resistant Staphylo- coccus aureus MRSA in a mouse rhinitis model. *Antimicrob. J. Chemother.* **2004**, *54*, 648–653.

[5] Heel, R.C.; Brogden, R.N.; Carmine, A.; Morley, P.A.; Speight, T.M.; Avery, G.S. Econazole: A review of its antifungal activity and therapeutic efficacy. *Drugs* **1982**, *23*, 1–36.

[6] Sheehan, D.J.; Hitchcock, C.A.; Sibley, C.M. Current and Emerging Azole Antifungal Agents. *Clin. Microbiol. Rev.* **1999**, *12*, 40–79.

[7] Lyman, C.A.; Walsh, T.J. Systemically Administered Antifungal Agents: A Review of Their Clinical Pharmacology and Therapeutic Applications. *Drugs* **1992**, *44*, 9–35.

[8] Clancy, C.J.; Nguyen, M.H. In vitro efficacy and fungicidal activity of voriconazole against Aspergillus and Fusarium species. *Eur. J. Clin. Microbiol. Infect. Dis.* **1998**, *17*, 573–575.

[9] Fung-Tomc, J.C.; Huczko, E.; Minassian, B.; Bonner, D.P. In Vitro Activity of a New Oral Triazole, BMS-207147 (ER-30346). *Antimicrob. Agents Chemother.* **1998**, *42*, 313–318.

[10] Espinel-Ingroff, A. Comparison of In Vitro Activities of the New Triazole SCH56592 and the Echinocandins MK-0991 (L-743,872) and LY303366 against Opportunistic Filamentous and Dimorphic Fungi and Yeasts. *J. Clin. Microbiol.* **1998**, *36*, 2950–2956.

[11] Khadri, M.J.N.; Begum, A.B.; Sunil, M.K.; Khanum, S.A. Synthesis, docking and biological evaluation of thiadiazole and oxadiazole derivatives as antimicrobial and antioxidant agents. *Results Chem.* **2020**, *2*, 100045.

[12] Holden, K.G. *Chemistry and Biology of b-Lactam Antibiotics*; Morin, R.B., Gorman, M., Eds.; Academic: London, UK, 1982; Volume 2, p. 114.

[13] Mata, E.G.; Fraga, M.A.; Delpiccolo, C.M.L. An Efficient, Stereoselective Solid-Phase Synthesis of β-Lactams Using Mukaiyama's Salt for the Staudinger Reaction. *J. Comb. Chem.* **2003**, *5*, 208–210.

[14] Pawar, R.P.; Andurkar, N.M.; Vibhute, Y.B. Studies on synthesis and antibacterial activity of some new Schiff bases, 4- thiazolidinones and 2-azetidinones. *J. Indian Chem. Soc.* **1999**, *76*, 271.

[15] Gootz, T.D. Discovery and development of new antimicrobial agents. *Clin. Microbiol. Rev.* **1990**, *3*, 13–31.

[16] Maiti, S.N. Overcoming bacterial resistance: Role of β-lactamase inhibitors. *Top. Heterocycl. Chem.* **2006**, *2*, 207–246.

[17] Singh, G.S. Beta-lactams in the new millennium. Part-I: Monobactams and carbapenems. *Mini-Rev. Med. Chem.* **2004**, *4*, 69.

[18] Singh, G.S. Beta-lactams in the new millennium. Part-II: Cephems, oxacephems, penams and sulbactam. *Mini-Rev. Med. Chem.* **2004**, *4*, 93.

[19] Risi, C.D.; Pollini, G.P.; Veronese, A.C.; Bertolasi, V. A new simple route for the

synthesis of (±)-2-azetidinones starting from β-Enaminoketoesters. *Tetrahedron Lett.* **1999**, *4*, 6995.

[20] Georg, G.I. (Ed.) *The Organic Chemistry of b-Lactams*; VCH: New York, NY, USA, 1993.

[21] Abdulla, R.F.; Fuhr, K.H. Monocyclic antibiotic beta-lactams. *J. Med. Chem.* **1975**, *18*, 625–627.

[22] Durckheimer, W.; Blumbach, J.; Lattrell, R.; Scheunemann, K.H. Recent developments in the field of b-lactam antibiotics. *Angew. Chem. Int. Ed. Engl.* **1985**, *24*, 180–202.

[23] Khanum, S.A.; Shashikanth, S.; Sudha, B.S. Microwave-Assisted Synthesis of 2-Amino and 2-Azetidinonyl 5-(2-Benzoyl- phenoxymethyl)-1,3,4-Oxadiazoles. *Het. Atom. Chem.* **2004**, *15*, 37.

[24] Khanum, S.A.; Shashikanth, S.; Sathyanarayana, S.G.; Lokesh, S.; Deepak, S.A. Synthesis and antifungal activity of 2-azetidinonyl- 5-(2-benzoylphenoxy)methyl-1,3,4-oxadiazoles against seed-borne pathogens of *Eleusine coracana* (L.) Gaertn. *Pest. Manag.* **2009**, *65*, 776–780.

[25] Banik, B.K.; Becker, F.F.; Banik, I. Synthesis of anticancer beta-lactams: Mechanism of action. *Bioorg. Med. Chem.* **2004**, *12*, 2523–2528.

[26] Gerona-Navarro, G.; de Vega, M.J.P.; Garcia-Lopez, M.T.; Andrei, G.; Snoeck, R.; de Clercq, E.; Balzarini, J.; Gonzalez-Muniz, R. From 1-acyl-β-lactam human cytomegalovirus protease inhibitors to 1-benzyloxycarbonylazetidines with improved antiviral activity. A straightforward approach to convert covalent. *J. Med. Chem.* **2005**, *48*, 2612–2621.

[27] Yoakim, C.; Ogilvie, W.W.; Cameron, D.R.; Chabot, C.; Guse, I.; Haché, B.; Naud, J.; O'Meara, J.A.; Plante, R.; Dé ziel, R. β-Lactam derivatives as inhibitors of human cytomegalovirus protease. *J. Med. Chem.* **1998**, *41*, 2882–2891.

[28] Alcaide, B.; Almendros, P. Selective Bond Cleavage of the β-Lactam Nucleus: Application in Stereo controlled Synthesis. *Synlett*, **2002**, *2022*, 381–393.

[29] Castagnolo, D.; Armaroli, S.; Corelli, F.; Botta, M. Enantioselective synthesis of 1-aryl-2-propenylamines: A new approach to a stereoselective synthesis of the Taxol®side chain. *Tetrahedron Asymmetry* **2004**, *15*, 941–949.

[30] Al-Ghorbani, M.; Thirusangu, P.; Gurupadaswamy, H.D.; Girish, V. Synthesis and antiproliferative activity of benzophenone tagged pyridine analogues towards activation of caspase activated DNase mediated nuclear fragmentation in Dalton's lymphoma. *Bioorg. Chem.* **2016**, *65*, 73–81.

[31] Neralagundi, H.G.S.; Begum, A.B.; Prabhakar, B.T.; Khanum, S.A. Design and synthesis of diamide-coupled benzophenones as potential anticancer agents. *Eur. J. Med. Chem.* **2016**, *115*, 342–351.

[32] Al-Ghorbani, M.; Thirusangu, P.; Gurupadaswamy, H.D.; Vigneshwaran, V. Synthesis of novel morpholine conjugated benzophe- none analogues and evaluation of antagonistic role against neoplastic development. *Bioorg. Chem.* **2017**, *71*, 55–66.

[33] Gulnaz, A.R.; Mohammed, Y.H.E.; Khanum, S.A. Design, synthesis, and molecular docking of benzophenone conjugated with oxadiazole sulphur bridge pyrazole pharmacophores as anti-inflammatory and analgesic agents. *Bioorg. Chem.* **2017**, *92*, 103220.

[34] Eissa Mohammed, Y.H.; Gurupadaswamy, H.D.; Khanum, S.A. Biological Evaluation of 2, 5-Di (4 Aryloylaryloxy Methyl)-1, 3, 4-Oxadiazoles Derivatives as Antimicrobial Agents. *Med. Chem.* **2017**, *7*, 837–843.

[35] Latha Rani, N.; Prashanth, T.; Zabiulla Sridhar, M.A.; Khanum, S.A. Structural Study and Antibacterial Activity of a Benzophenone Derivative: [2-Bromo-4-(2-chloro-benzoyl)-phenoxy]-acetic acid ethyl ester. *J. Appl. Chem.* **2016**, *5*, 628–636.

[36] Azoro, C. Antibacterial activity of crude extract of Azadiracta indica on Salmonella typhi. *World J. Biotechnol.* **2002**, *3*, 347–357.

[37] Chung, K.T.; Thomasson, W.R.; Wu-Yuan, C.D. Growth inhibition of selected food-borne bacteria, particularly Listeria monocyto- genes, by plant extracts. *J. Appl. Bacteriol.* **1990**, *69*, 498–503.

[38] Janovska, D.; Kubikova, K.; Kokoska, L. Screening for antimicrobial activity of some medicinal plants species of traditional Chinese medicine. *J. Food Sci.* **2003**, *21*, 107–110.

[39] Bishnu, J.; Sunil, L.; Anuja, S. Antibacterial Property of Different Medicinal Plants: Ocimum sanctum, Cinnamomum zeylanicum, Xanthoxylum armatum and Origanum majorana, Kathmandu university journal of science engineering and technology. *J. Sci. Eng. Technol.* **2009**, *5*, 143–150.

[40] Clinical and Laboratory Standards Institute. *Methods for Dilution Antimicrobial Susceptibility Tests for Bacteria That Grow Aerobically*, 7th ed.; National Committee for Clinical Laboratory Standards; Approved Standard, CLSI Document M7-A7; Clinical and Laboratory Standards Institute: Wayne, PA, USA, 2006.

[41] Clinical and Laboratory Standards Institute. *Reference Method for Broth Dilution Antifungal Susceptibility Testing of Yeasts*, 2nd ed.; National Committee for Clinical Laboratory Standards; Proposed Standard, NCCLS Document M27-A2; Clinical and Laboratory Standards Institute: Wayne, PA, USA, 2002.

[42] Morris, G.M.; Huey, R.; Lindstrom, W.; Sanner, M.F.; Belew, R.K.; Goodsell, D.S.; Olson, A.J. AutoDock4 and AutoDockTools4: Automated

docking with selective receptor flexibility. *J. Comput. Chem.* **2009**, *30*, 2785–2791.

[43] Morris, G.M.; Goodsell, D.S.; Halliday, R.S.; Huey, R.; Hart, W.E.; Belew, R.K.; Olson, A.J. Automated docking using a Lamarckian genetic algorithm and an empirical binding free energy function. *J. Comput. Chem.* **1998**, *19*, 1639–1662.

[44] Khamees, H.A.; Jyothi, M.; Khanum, S.A.; Madegowda, M. Synthesis, crystal structure, spectroscopic characterization, docking simulation and density functional studies of 1-(3,4-dimethoxyphenyl)-3-(4-flurophenyl)-propan-1-one. *J. Mol. Struct.* **2018**, *1161*, 199–217.

[45] Carr, R.A.; Congreve, M.; Murray, C.W.; Rees, D.C. Fragment-based lead discovery: Leads by design. *Drug Discov. Today* **2005**, *10*, 987–992.

[46] Shultz, M.D. improving the plausibility of success with inefficient metrics. *ACS Med. Chem. Lett.* **2014**, *5*, 2–5.

[47] Abad, N.; Sallam, H.H.; Al-Ostoot, F.H.; Khamees, H.A.; Al-horaibi, S.A.; Sridhar, M.A.; Khanum, S.A.; Madegowda, M.; El-hfi, M.; Maque, J.T.; et al. Synthesis, crystal structure, DFT calculations, Hirshfeld surface analysis, energy frameworks, molecular dynamics and docking studies of novel isoxazolequinoxaline derivative (IZQ) as anti-cancer drug. *J. Mol. Struct.* **2021**, *1232*, 130004.

[48] Biovia, D.S. Discovery Studio Visualiser v19.10.18287, 2018 (San Diego, CA, USA). (accessed on 20 September 2022).

[49] *The PyMOL Molecular Graphics System, 2015*; Version 2.0; Schrodinger, LLC: New York, NY, USA, 2015.

[50] Mehta, P.D.; Sengar, N.P.; Pathak, A.K. 2-Azetidinone—A new profile of various pharmacological activities. *Eur. J. Med. Chem.* **2010**, *45*, 5541–5560.

[51] Bush, K.; Bradford, P.A. β-Lactams and β-Lactamase Inhibitors: An Overview. *Cold Spring Harb. Perspect. Med.* **2016**, *6*, a025247.

[52] Al-Ghorbani, M.; Lakshmi Ranganatha, V.; Prashanth, T.; Begum, B.; Khanum, S.A. In vitro antibacterial and antifungal evaluation of some benzophenone analogues. *Der Pharma Chem.* **2013**, *5*, 269–273.

[53] Prashanth, T.; Naveen, P.; Al-Ghorbani, M.; Asha, M.S.; Khanum, S.A. Synthesis and Inhibition of Microbial Growth by Benzophenone Analogues—A Simplistic Approach. *Asian J. Biomed. Pharm. Sci.* **2014**, *4*, 55–60.

[54] Lakshmi Ranganatha, V.; Khanum, N.F.; Khanum, S.A. Synthesis, and evaluation of in vitro anti-microbial properties of novel benzophenone tagged indole analogues via 1, 3, 4-oxadiazole linkage. *Int. J. Med. Pharm. Sci.* **2013**, *3*, 97–106.